

Ride-pooling Electric Autonomous Mobility-on-Demand: Joint Optimization of Operations and Fleet and Infrastructure Design

Fabio Paparella^{a,*}, Karni Chauhan^a, Luc Koenders^a, Theo Hofman^a, Mauro Salazar^a

^aControl Systems Technology section, Eindhoven University of Technology, the Netherlands

Abstract

This paper presents a modeling and design optimization framework for an Electric Autonomous Mobility-on-Demand system that allows for ride-pooling, i.e., multiple users can be transported at the same time towards a similar direction to decrease vehicle hours traveled by the fleet at the cost of additional waiting time and delays caused by detours. In particular, we first devise a multi-layer time-invariant network flow model that jointly captures the position and state of charge of the vehicles. Second, we frame the time-optimal operational problem of the fleet, including charging and ride-pooling decisions as a mixed-integer linear program, whereby we jointly optimize the placement of the charging infrastructure. Finally, we perform a case-study using Manhattan taxi-data. Our results indicate that jointly optimizing the charging infrastructure placement allows to decrease overall energy consumption of the fleet and vehicle hours traveled by approximately 1% compared to an heuristic placement. Most significantly, ride-pooling can decrease such costs considerably more, and up to 45%. Finally, we investigate the impact of the vehicle choice on the energy consumption of the fleet, comparing a lightweight two-seater with a heavier four-seater, whereby our results show that the former and latter designs are most convenient for low- and high-demand areas, respectively.

Keywords: Autonomous mobility-on-demand, electric vehicles, ride-pooling, transportation systems.

1. Introduction

Recent advances in autonomous driving and powertrain electrification are paving the way to the deployment of Electric Autonomous Mobility-on-Demand (E-AMoD) systems as shown in Fig. 1, whereby electric self-driving robo-taxis provide on-demand mobility. In this context, both operational aspects such as vehicle routing, rebalancing, ride-pooling and charge scheduling, and design aspects such as vehicle design in terms of battery capacity and number of seats, and charging infrastructure placement, have a strong impact on the achievable performance, whilst also being intimately coupled: For instance, the battery capacity of the vehicles and the charging infrastructure placement influence the fleet operation in terms of routing and charge scheduling, whilst the number of seats constrain the implementable ride-pooling schemes and dictate the energy consumption, which in turn, influence the vehicle hours traveled (VHT) and charging schedules. Therefore, all the aforementioned design and operational aspects should be jointly optimized when deploying E-AMoD systems. This paper proposes an optimization framework to optimize the planning of an E-AMoD system that allows for ride-pooling, jointly with the placement of the charging infrastructure, whilst minimizing the fleet size in a computationally efficient and tractable manner. The proposed framework allows to rapidly explore a large design space, which is a desirable feature when comparing, for example, different vehicle's architectures and fleet compositions.

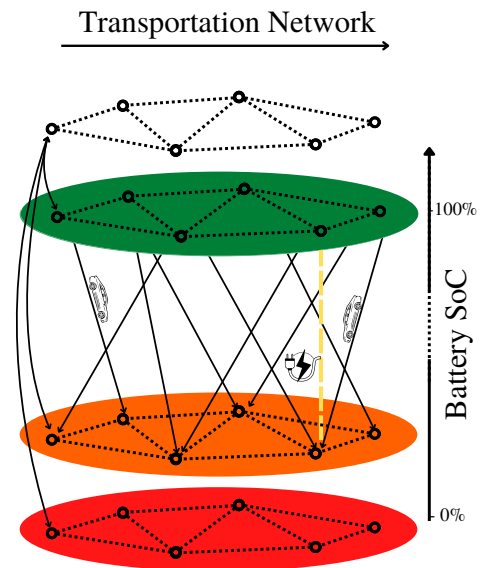


Figure 1: Multi-layer network schematically representing an E-AMoD system. Each layer corresponds to a battery state of charge (SoC). The top layer represents the original network where each node, called geo-node, represents a geographical location. The curved geo-arcs connect every layer to the same geographical location. As a car travels, it drives through the solid arcs and decrease its SoC. The yellow arcs are placed at charging stations and capture charging activities.

*Corresponding author.

Email address: f.paparella@tue.nl (Fabio Paparella)

ing and charging infrastructure siting.

A multitude of approaches to model and control AMoD systems are available (Banerjee et al., 2015; Iglesias et al., 2019; Levin et al., 2017; Hoppe et al., 2024; Turan et al., 2019; Alizadeh et al., 2014; Le Floch et al., 2015). In particular, multi-commodity network flow models (Spieser et al., 2014; Pavone, 2015) are ideal for design optimization purposes as they do not scale with the number of vehicles, and allow for the implementation of multiple objectives and constraints, such as the minimization of VHT by the fleet.

Ride-pooling was studied in recent years. In Santi et al. (2014), the authors analyzed the benefits of pooling, while in Alonso-Mora et al. (2017) they developed an algorithm that can solve the ride-pooling problem in an optimal manner with high capacity vehicles. However, these microscopic frameworks are computationally very expensive, and cannot be directly leveraged for design optimization purposes. Against this backdrop, we recently proposed a linear network flow modeling approach that allows to study ride-pooling AMoD from a mesoscopic planning perspective (Paparella et al., 2024c), also accounting for endogenous congestion (Paparella et al., 2024b), but not including electric vehicles.

Finally, the deployment of electric vehicles introduce the energy consumption and charging dimension, and was studied with directed acyclic graphs in Boewing et al. (2020); Paparella et al. (2024a), which can also be leveraged for other electric mobility problems such as freight transportation (Wang et al., 2023; Bertucci et al., 2024) and electric air mobility (Vehlhaber and Salazar, 2023). Mesoscopic planning models were studied accounting for the interaction with the power grid in (Rossi et al., 2020; Estandia et al., 2021), whilst a time-varying E-AMoD model was proposed in Luke et al. (2021) that allows to jointly optimize the operations and charging infrastructure for an E-AMoD system, however at the cost of large computational efforts for relatively small and clustered road networks, and without accounting for ride-pooling.

In conclusion, to the best of the authors' knowledge, there are no mesoscopic models available to optimize the operations of an E-AMoD fleet with ride-pooling, jointly with the charging infrastructure siting in a computationally-tractable manner and with global optimality guarantees.

Statement of Contributions: This paper presents a modeling and optimization framework to jointly optimize the ride-pooling and charging operations of an E-AMoD fleet jointly with the charging infrastructure placement in a computationally-effective manner and with global optimality guarantees. First, we propose a linear time-invariant network flow model capturing the fleet routing including ride-pooling and charging activities, and combine it with the combinatorial infrastructure design problem. Second, we frame the optimization problem as a mixed-integer linear program that can be efficiently solved with off-the-shelf optimization algorithms. Finally, we showcase our framework with two case studies in Manhattan, NYC, USA.

A preliminary version of this paper was presented at the 2023 IFAC World Congress (Paparella et al., 2023). In this extended version, we include the ride-pooling capabilities of the frame-

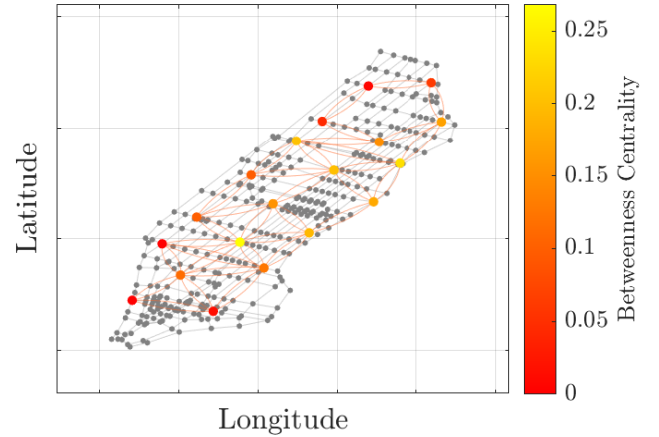


Figure 2: Original road network of Manhattan (grey). Pruned synthetic network (colored) with equal (energy) weights.

work, that allow to study the performance of the system as a function of the maximum waiting time and delay experienced by the users. In addition, we develop a pruning algorithm that allows to transform a road network in a synthetic road network with iso-energy consumption arcs, which enables a significant decrease in the computational complexity of the problem. Finally, we study the performance achievable by different electric vehicles.

Organization: The remainder of this paper is structured as follows: Section 2 devises the E-AMoD modeling and optimization framework. Section 3 presents our case studies for Manhattan, NY. Finally, Section 4 draws the conclusions and provides an outlook on future research.

2. Methodology

In this section, we present a multi-layer time-invariant network flow model to optimize the operation of an E-AMoD system with ride-pooling jointly with the placement of the charging infrastructure, Fig. 1.

2.1. Multi-layer Network

We model the transportation network as a directed graph $\mathcal{G}_R = (\mathcal{V}_R, \mathcal{A}_R)$ with a set of nodes \mathcal{V}_R representing the location of intersections on the road network, and a set of arcs \mathcal{A}_R representing the road link between connected nodes. Each road arc $(i, j) \in \mathcal{A}_R$ is characterized by a distance d_{ij} , travel time t_{ij} , and energy e_{ij} required to traverse it.

To model the SoC of the fleet, we build a multi-layer network $\mathcal{G} = (\mathcal{V}, \mathcal{A})$, where each layer has the same set of nodes of the original road network \mathcal{V}_R . Fig. 1 shows a schematic representation of the multi-layer network. Each node in each layer has a set of "copy nodes" in the other layers that represent the same geographical location, but indicate a different SoC. The first layer indicates the battery at 100%, the last layer at 0% SoC, and the number of layers n depends on the discretization of the SoC of the battery. We define the set of nodes of the multi-layer network as the union of the set of nodes in every layer,

$\mathcal{V} = \mathcal{V}_1 \cup \mathcal{V}_2 \cup \dots \cup \mathcal{V}_n$. As vehicles commute each arc, they also move to a lower layer, representing the depleting SoC. This is reflected in a new set of directed arcs \mathcal{A} such that a node in a given layer is connected with a node in a layer below, i.e., with a lower SoC. In fact, nodes in the same layer are not connected because it would mean vehicles traveling without spending energy. As a consequence, the new set of arcs \mathcal{A} can only connect nodes in different layers so that the energy spent is reflected in an equivalent number of layers traversed down.

2.2. Travel Requests and Charging Stations

On top of the multi-layer network, we introduce a set of geo-nodes \mathcal{V}_G . Every geo-node is connected via geo-arcs \mathcal{A}_G to every other node that represents the same geographical location, across all the battery SoC layers. Geo-arcs have zero weight because they connect nodes that represent the same geographical location. We define as $\mathcal{G} = (\mathcal{V}, \mathcal{A})$ the multi-layer network comprehensive of geo-nodes and arcs. Then, we define $\mathcal{M} = \{1, \dots, M\}$ as a set of travel requests. Each request $m \in \mathcal{M}$ is defined by a tuple $r_m = (o_m, d_m, \alpha_m) \in \mathcal{V}_G \times \mathcal{V}_G \times \mathbb{R}^+$ in which α_m is the number of users traveling from the origin o_m to the destination d_m per unit time. Note that travel requests are initialized on \mathcal{V}_G .

The user flow induced by each demand m is defined as x_{ij}^m , with $m \in \mathcal{M}$ and $(i, j) \in \mathcal{A}$. All user demand flows x_{ij}^m are fulfilled by vehicles, and the rebalancing vehicle flows are defined as x_{ij}^r , which we define as the flow on arc $(i, j) \in \mathcal{A}$ of vehicles without users on-board. Both the user demand flow and the rebalancing flow originate and terminate in a geo-node in the set \mathcal{V}_G . We define a set of potential charging station locations as $C \subset \mathcal{V}_G$, with charging station $c \in C = \{1, 2, \dots, |C|\}$. We define a vector with binary entry κ_c indicating with $\kappa_c = 1$ if there is a charging station at node c , and $\kappa_c = 0$ otherwise. A charging station c is modeled as a set of charging arcs \mathcal{A}_S^c , which allows the vehicles inside a charging station c to move from a layer to the subsequent layer above, while remaining at the same geographic location. Vehicles can only be charged while rebalancing via charging arcs $(i, j) \in \mathcal{A}_S^c, \forall c \in C$. Hence, we extend the multi-layer network \mathcal{G} by including the set of charging arcs $(i, j) \in \mathcal{A}_S^c$.

2.3. Pruning of the Multi-layer Network with Iso-energy Arcs

While vehicles travel they also deplete SoC, meaning that they have to traverse down an equivalent amount of energy w.r.t. the distance driven. However, due to the discretization of the SoC, it is not guaranteed to have an exact match between distance traveled and energy used. In particular, given the wide range of arc lengths and their relative energy consumption, the SoC discretization should be extremely fine, i.e., the number of layers should be very large, to avoid such mismatches. Crucially, the complexity of a traffic flow model grows with the square of the number of nodes. In addition, when jointly optimizing for the siting of the charging infrastructure, the combinatorial nature of the formulation can potentially lead to either intractable problems or the necessity of large computational resources. Moreover, it is desirable to have a formulation that

allows for the computation of the solution in a reasonable time period. This is the case when a large design space of the base vehicle has to be explored and tested. Thus, we devise an algorithmic procedure to transform the original road network into a new synthetic network with iso-energy arcs. In other words, the new synthetic network has the characteristic of having arcs with equal weight in terms of energy consumption, while minimizing the absolute error of the shortest path distance w.r.t. the original network. The full procedure can be found in Appendix A. The contribution of this procedure is twofold: i) it decreases the number of nodes in every layer, while minimizing the errors caused by the pruning; ii) the constant weight allows for an exact match between distance traveled and energy consumed and consequently a reduction in the number of SoC layers needed.

2.4. Network Flow Model Formulation

We set as objective the minimization of the number of vehicles, which is equivalent of minimizing the total travel time of the fleet (Pavone, 2015):

$$\min_{x^m, x^r} \sum_{m \in \mathcal{M}} \sum_{(i,j) \in \mathcal{A}} t_{ij} \cdot (x_{ij}^m + x_{ij}^r), \quad (1)$$

where x_{ij}^m is the user demand flow, x_{ij}^r is the rebalancing flow, t_{ij} is the time to traverse arc $(i, j) \in \mathcal{A}$. Note that this objective is equivalent to the minimization of the number of vehicles required to implement the obtained flows, as demonstrated by Pavone et al. (2012). The vehicle and user flow conservation are expressed as in a multi-commodity transportation problem

$$\sum_{(i,j) \in \mathcal{A}} x_{ij}^m + \mathbb{1}_{j=o_m} \cdot \alpha_m = \sum_{(j,k) \in \mathcal{A}} x_{jk}^m + \mathbb{1}_{j=d_m} \cdot \alpha_m \quad \forall m \in \mathcal{M}, \quad (2)$$

where the user flow x_{ij}^m is induced by demand m , $\mathbb{1}_{x=y}$ is the indicator function, equal to 1 if $x = y$ and zero otherwise, and α_m is the user request rate per unit time. Rebalancing the vehicles in the E-AMoD system is critical to create a balanced system and to realign vehicle distribution with transportation requests. This is ensured by

$$\sum_{(i,j) \in \mathcal{A}} \left(x_{ij}^r + \sum_{m \in \mathcal{M}} x_{ij}^m \right) = \sum_{(j,k) \in \mathcal{A}} \left(x_{jk}^r + \sum_{m \in \mathcal{M}} x_{jk}^m \right). \quad (3)$$

The geo-nodes in \mathcal{V}_G act as origins and destinations for the vehicles. Consequently, each demand will require the geo-arcs \mathcal{A}_G to be used twice: first, from a geo-node to the road network, and then from the road network to a geo-node. The same is also applicable to rebalancing flows. This is ensured by constraining the user flow by

$$\sum_{m \in \mathcal{M}} \left(\sum_{(i,j) \in \mathcal{A}_G} x_{ij}^m + \sum_{(k,l) \in \mathcal{A}_G} x_{kl}^m \right) = 2 \cdot \sum_{m \in \mathcal{M}} \alpha_m \quad \forall i, l \in \mathcal{V}_G, \quad (4)$$

and the rebalancing flows to

$$\sum_{(i,j) \in \mathcal{A}_G} x_{ij}^r + \sum_{(k,l) \in \mathcal{A}_G} x_{kl}^r = 2 \cdot \sum_{m \in \mathcal{M}} \alpha_m \quad \forall i, l \in \mathcal{V}_G. \quad (5)$$

We enforce SoC conservation when passing through a geo-node \mathcal{V}_G as

$$\sum_{(i,j) \in \mathcal{A}_G} x_{ij}^m - x_{ji}^r = 0 \quad \forall m \in \mathcal{M}, \forall i, j \in \mathcal{V}_G. \quad (6)$$

We also impose the set of possible charging stations locations $C = \mathcal{V}_G$ and set the limit of the number of charging stations to $N \in \mathbb{N}$ with

$$\sum_{c=1}^{|C|} \kappa_c \leq N. \quad (7)$$

Each charging station has a limited capacity in terms of the number of vehicles it can charge simultaneously. The capacity constraint of each charging station is given by

$$\Delta E \cdot \sum_{(i,j) \in \mathcal{A}_S^c} x_{ij}^r \leq P_{\max} \quad \forall c \in C, \quad (8)$$

where P_{\max} is the charging station power, and ΔE is the difference in SoC between the layers, which is a constant and which limits the rebalancing flow through the charging arcs $(i, j) \in \mathcal{A}_S^c$. Since the vehicles must not charge with users on-board, the charging of the vehicles can be carried out only while rebalancing. This is ensured by

$$x_{ij}^m = 0 \quad \forall m \in \mathcal{M}, \forall (i, j) \in \mathcal{A}_S^c, \quad (9)$$

which guarantees that the vehicles do not charge when serving users. Therefore, the vehicles can only charge while rebalancing through charging arcs $(i, j) \in \mathcal{A}_S^c$. Then, we impose non-negative flow constraints,

$$x_{ij}^r \geq 0 \quad \forall (i, j) \in \mathcal{A}, \quad (10)$$

$$x_{ij}^m \geq 0 \quad \forall m \in \mathcal{M}, \forall (i, j) \in \mathcal{A}. \quad (11)$$

To conclude, we define the E-AMoD optimization problem as follows:

Problem 1. (E-AMoD Joint Optimization Problem) Given a set of transportation requests \mathcal{M} , the optimal user flows x^m , the rebalancing flows x^r , and the optimal siting of the charging infrastructure c , result from

$$\begin{aligned} \min_{x^m, x^r, c} & \sum_{m \in \mathcal{M}} \sum_{(i,j) \in \mathcal{A}} t_{ij} \cdot (x_{ij}^m + x_{ij}^r), \\ \text{s.t.} & \quad (2) - (11). \end{aligned}$$

Problem 1 is a mixed-integer linear program (MILP) that can be solved with global optimality guarantees with off-the-shelf solvers. In addition, given a pre-defined set of charging stations, the problem can be cast as a linear program that can be efficiently solved with interior-point algorithms in polynomial time.

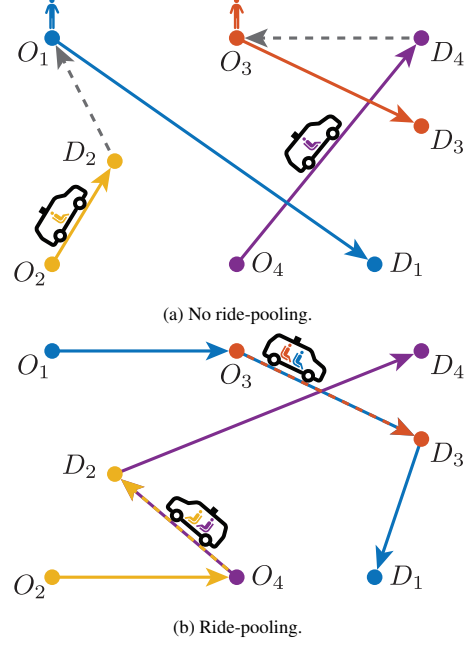


Figure 3: Illustrative example of no ride-pooling and ride-pooling with two vehicles; dashed arrows indicate vehicles traveling without users on-board. Figure taken from Paparella et al. (2024c).

2.5. Ride-pooling Network Flow Model Formulation

In the previous section, the standard network flow model formulation was presented. One of the main assumptions of the model is that each vehicle can only transport one user at the time. However, the replacement of private vehicles with an AMoD fleet can lead to an increase in VHT due to the rebalancing term. Thus it is crucial to include ride-pooling, which is schematically depicted in Fig. 3, allowing two or more users to travel on a vehicle at the same time. Given the combinatorial nature of the problem, it is important to find a method that is reasonably fast, in line with the method of this work. Given a set \mathcal{M} of travel requests in a time-invariant network flow model, it is possible to compute an equivalent set of travel requests \mathcal{M}' that includes the possibility for users to ride-pool, which is optimal w.r.t. the VHT by the fleet with users on-board. In particular, the new set can be computed for as a function of the maximum waiting time \bar{t} , a maximum delay $\bar{\delta}$, and a maximum vehicle capacity K , which are the maximum waiting time a user is willing to wait another user, the maximum time caused by the detour w.r.t. no ride-pooling, and the maximum number of users that can be pooled together in the same vehicle at the same time, respectively. Given the new set \mathcal{M}' , it is possible to solve Problem 1 while taking into account ride-pooling. The idea has been proposed in Paparella et al. (2024c), which we refer to the reader for a detailed analysis. In what follows, we briefly explain the methodology. For the sake of simplicity, we restrict the number of users that can ride-pool together to $K = 2$. Nonetheless, the reasoning can be applied to any K , as detailed in the aforementioned work. Given three travel requests $r_1 = (o_1, d_1, \alpha_1)$, $r_2 = (o_2, d_2, \alpha_2)$ and $r_3 = (o_3, d_3, \alpha_3)$, there are nine ways in which it is possible to ride-pool such travel re-

quests, corresponding to the combinations between them (with repetitions and with permutations). In each ordered combination there is one way to pick up travel requests and one way to drop them off that minimizes the vehicle hour traveled by the fleet. For example, to ride-pool r_1 and r_2 (in that order), a vehicle should travel through the nodes o_1, o_2 in that order and then, starting from o_2 , to d_1, d_2 in the order that minimizes the VHT. To force the vehicle to travel through those nodes, the ride-pooling travel request between r_1, r_2 can be represented by an equivalent set composed by three travel requests that would force a vehicle to first pick-up both the requests and then drop them off. An example would be:

$$r_{12}^1 = (o_1, o_2, \min(\alpha_1, \alpha_2)P(\alpha_1, \alpha_2, \bar{t}))$$

$$r_{12}^2 = (o_2, d_1, \min(\alpha_1, \alpha_2)P(\alpha_1, \alpha_2, \bar{t}))$$

$$r_{12}^3 = (d_1, d_2, \min(\alpha_1, \alpha_2)P(\alpha_1, \alpha_2, \bar{t})),$$

where $r_{12}^1, r_{12}^2, r_{12}^3$ are the equivalent travel requests that would force the vehicle to pass through o_1, o_2, d_1, d_2 . The $\min(\cdot)$ imposes that the same number of users from both travel requests are taken, the function $P(\alpha_1, \alpha_2, \bar{t})$ is a probability function of having one single user from the travel request r_1 and one from r_2 within a time window \bar{t} and it is given, for a generic number of k travel requests, by

$$P_{\bar{t}}(\alpha_1, \dots, \alpha_k) = \sum_{i=1}^k \frac{\alpha_i}{\sum_{j=1}^k \alpha_j} \prod_{\substack{j=1 \\ j \neq i}}^k (1 - e^{-\alpha_j \bar{t}}). \quad (12)$$

Thus, for a given r_1, r_2 the equivalent set of ride-pooling travel requests composed by $r_{12}^1, r_{12}^2, r_{12}^3$ can be fully defined. Note that the probability given by (12) is always strictly lower than 1, meaning that two travel requests cannot be fully ride-pooled together, i.e., some users cannot be ride-pooled due to time constraints. The remaining part of such users that could not be pooled can, however, potentially be pooled with other travel requests. In the previous example, the remaining users from r_1, r_2 can be pooled with the users from r_3 . This second step is dependent on the previous step, as it depends on how many users remain unmatched from the original travel requests r_1, r_2 after the previous step. In addition, the order of matching r_1, r_3 and r_2, r_3 influences the final result. The priority has to be optimized accordingly to minimize the objective, which in this case is the VHT with users on-board. This procedure leads to a non-linear mixed integer problem, which can quickly become untractable, even for a small number of travel requests. To solve this problem in an efficient way, we leverage a Knapsack-like algorithm, which has been proved to be optimal w.r.t. the VHT by the fleet with users on-board (Paparella et al., 2024c, Theorem 1). The algorithm allows to prioritize the ride-pooling matches and allows to solve the problem in polynomial time. The equivalent set of travel requests obtained represents the expected number of ride-pooling matches that can be performed under maximum waiting time \bar{t} and detour $\bar{\delta}$ constraints. Problem 1 with the new set \mathcal{M}' allows to solve the minimum VHT problem.

2.6. Discussion

A few comments are in order. First, we model the system at steady-state. This assumption holds if the rate change of requests is significantly lower than the average travel time of individual trips, as observed in densely populated urban environments by Neuburger (1971). In addition, vehicle conservation implicitly enforces SoC conservation over the time-span under consideration. Second, the iso-energy synthetic network procedure is only valid for environments where traveling to and from a node requires approximately the same amount of energy, e.g., flat urban environments. In the future, the authors intend to extend this model to capture more general (e.g., hilly) scenarios as well. Third, the results obtained by solving Problem 1 allow for fractional flows to occur. This is acceptable given the mesoscopic nature of the problem, where arc flows are in the order of hundreds of vehicles, see Luke et al. (2021). However, it is possible to retrieve near-optimal integer flows from fractional ones leveraging randomized sampling methods, as shown by Rossi et al. (2017). Fourth, we do take into account the exogenous traffic and its stochastic nature for a specific traffic scenario. In case of different conditions, the travel time and energy consumption can be updated accordingly, and a new synthetic network can be generated. Finally, we neglect the effect of endogenous traffic and the reaction of private vehicles. However, it is possible to readily account for exogenous traffic congestion by modifying the entries t_{ij} accordingly.

3. Results

We investigate two case studies for the metropolitan region of Manhattan, NYC. The original data set is extracted from OpenStreetMap, whilst to create the synthetic network we leverage the algorithm explained in Section 2.3. Following the results in Appendix A, we set the target weight to 100 Wh and the compression rate to 90%. The travel requests are publicly available from the website of the New York Taxi commission. The data set used as a reference is the peak-hour from 8 to 9AM during March 1st, 2022, which has approximately 14'000 travel requests. We investigate two case studies. The first one assesses the advantages of jointly optimizing the infrastructure siting w.r.t. a heuristic placement based on geo-nodes centrality. In particular, we analyze the impact of the charging infrastructure density and siting on the resulting rebalancing flow energy consumed by the whole fleet. Then, we investigate the benefit that ride-pooling has on sizing of the charging infrastructure. The second case study evaluates the performance of the E-AMoD system when different designs of electric vehicles in terms of battery capacity, passenger seats, and efficiency per unit distance driven are employed, see Table 1. The three vehicles are a small 2-seater, which has the smallest battery capacity and the lowest energy consumption, a medium 4-seater, with a larger battery capacity and a higher energy consumption, and a 4-seater+, which has the highest battery capacity, making it the heaviest and most energy-consuming one.

Table 1: Normalized Parameters of the Vehicles under Consideration.

	2-seater	4-seater	4-seater+
Energy consumption	85%	93%	100%
Battery capacity	25%	60%	100%
Mass	69%	85%	100%
Number of Seats	2	4	4

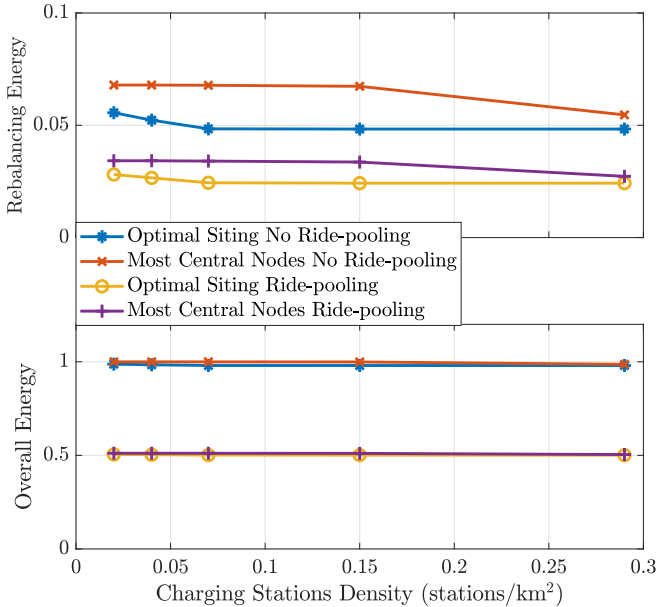


Figure 4: The rebalancing and overall energy consumption for the whole fleet leveraging an optimal approach and an heuristic method, betweenness centrality, to do the siting of the charging infrastructure for Manhattan, NYC. Results are both with and without ride-pooling scenario, with a maximum of two users per vehicle at the same time, $K = 2$. The results are normalized w.r.t. the overall energy usage of the no ride-pooling scenario with heuristic placement.

3.1. Charging Infrastructure Design

In this case study we investigate the impact of the charging infrastructure density, siting, sizing and of ride-pooling on the energy consumption of a fleet of 4-seaters, but where we restrict the maximum number of users that can be ride-pooled together to $K = 2$. We assess the advantages of jointly optimizing siting and routing by comparing the results of Problem 1 w.r.t. the same framework, but where the siting of the charging infrastructure is selected a priori leveraging an heuristic approach. Namely, we use the *betweenness* centrality, Bullo (2020), i.e., we place the charging stations in the nodes with the highest probability of appearing on the shortest path between any two random nodes, as shown in Fig. 2. As an alternative, other methods like k-mean clustering could be implemented. Fig. 4 shows the normalized overall and rebalancing energy usage in four scenarios for a varying density of charging stations per unit area. The four scenarios are with and without ride-pooling, and with optimal and heuristic placement. For the ride-pooling scenarios we set the maximum waiting time and the maximum delay of users to $\bar{\delta}, \bar{\tau} = 10$ min, and the maximum number of users that can ride-pool together to $K = 2$. We recall that the waiting

time is the time that a user is willing to wait for another user to be pooled together, and delay is the additional detour time w.r.t no pooling. We notice that when going for the optimal siting of the charging infrastructure, it is possible to decrease the overall energy consumption of the fleet by approximately 1% compared to heuristic placement in both the cases of ride-pooling and no ride-pooling. Such improvement is significantly lower compared to the one given by allowing for ride-pooling. In fact, given that users can share vehicles at the same time, a lower number of vehicles is required and the overall total energy is significantly reduced. When comparing rebalancing energy consumption per vehicle, the results are very similar between ride-pooling and no ride-pooling. In addition, when performing ride-pooling, the optimal placement remains the same, and the rebalancing flow patterns do not vary significantly. As a result, when designing the siting of the charging infrastructure in a ride-pooling framework, it is possible to leverage state-of-the-art methodologies for mobility systems that do not account for ride-pooling. The results show that above a density of 0.1 stations/km², if the siting is optimal, we reach a plateau. Up to this point, assuming each station is large enough to always have free charging spots, it is not convenient to build additional stations. On the contrary, by using the betweenness centrality heuristic method, the number of charging stations needs to increase to obtain a similar performance. In contrast with siting, sizing is strongly dependent on the decision of allowing for ride-pooling or not. Fig. 5 shows the improvement of overall energy usage of ride-pooling w.r.t. no ride-pooling. Interestingly, increasing the delay does not significantly improve the energy consumption, as the vehicles perform more detours to pick-up and drop-off users. On the contrary, waiting time strongly impacts energy consumption because users and vehicles waiting implies no energy consumption. The results show that ride-pooling can lead to a significant decrease in energy usage, in the order of 45%, even for small maximum waiting time and delay experienced by users. This result is mainly due to the very large number of travel requests that occur in Manhattan, which allows for an efficient matching of users. However, different regions with lower number of travel requests will experience a lower improvement. We refer to Paparella et al. (2024c) for a detailed analysis on the correlation between improvement in VHT, which can be directly correlated to energy consumption and number of travel requests.

3.2. Impact of the Vehicle Design on the Optimal Operations

This section shows a second case study where we assess the impact of vehicles' characteristics on the performance of the E-AMoD system. Specifically, we select three different commercial vehicles of which the normalized parameters are shown in Table 1. The parameters of these vehicles are normalized w.r.t. the LightYear One (Lightyear, 2016). Following the results of Section 3.1, we solve Problem 1 with an optimally sited charging infrastructure of density equal to 0.1 stations/km². We perform a simulation for every type of vehicle, both with and without ride-pooling with a maximum delay and waiting time of $\bar{\delta}, \bar{\tau} = 10$ min and a maximum of two users per vehicle at the same time, $K = 2$. Then, we analyze the differences in

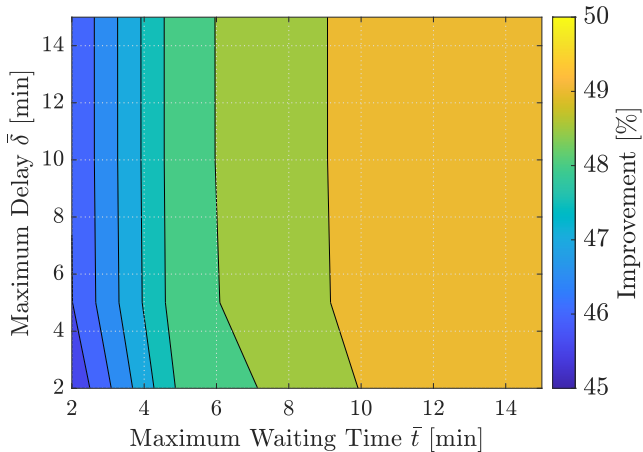


Figure 5: Improvement of overall daily energy usage of the ride-pooling scenario w.r.t. no pooling, for a varying waiting time and delay \bar{t} and $\bar{\delta}$, respectively. Seat capacity of the vehicles $K = 2$. Overall number of demands equal to 14 thousand per hour. All charging stations have the same power available.

terms of the user flow and rebalancing flow energy consumption, as illustrated in Fig. 6. We highlight that the rebalancing flow distance in the three cases with different vehicles is the same and that the difference in energy consumption is mainly due to the difference in consumption per unit distance driven. This result is in line with the results obtained by Hogeveen et al. (2021); Paparella et al. (2024a), which show that in mobility-on-demand frameworks, vehicles with battery capacity above a certain threshold have a comparable rebalancing flow distance traveled (including detour to charging stations). First, our results indicate that when choosing vehicles for mobility-on-demand, it is important to give priority to efficiency in terms of consumption per unit distance driven compared to battery capacity. In fact, the majority of commercial vehicles have a battery capacity which is above a threshold, which results in approximately constant rebalancing distance. Second, we highlight that allowing for ride-pooling leads to a significant decrease in overall distance driven and energy consumed. This is especially the case in a densely populated urban environment where it is possible to efficiently and conveniently match together the majority of the travel requests. In what follows, we will compare the performance of the 2-seater and the 4-seater for a varying number of travel requests, and allowing users to be ride-pooled together up to the number of seats in each vehicle, i.e., $K = 2, 4$, respectively. We disregard the 4-seater+ as we have shown that the additional battery capacity does not lead to any improvement. Fig. 7 shows the ratio of overall energy consumption between a fleet of 2-seaters and 4-seaters where it is possible to ride-pool users up to the number of seats in the vehicles. The results indicate that it is not always convenient to choose the smallest vehicles, but that the design choice is strongly influenced by both the number of travel requests and the maximum waiting time \bar{t} that users are willing to withstand. In fact, for a low maximum waiting time \bar{t} and a low number of travel requests, pooling more than two users is very unlikely and inefficient. As a consequence, the higher efficiency of the 2-

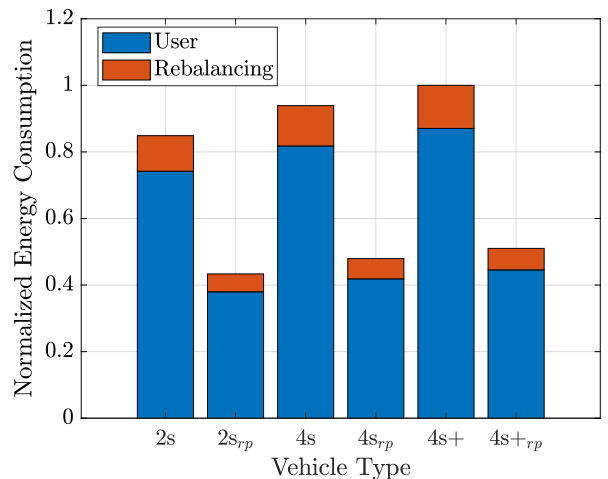


Figure 6: Energy used by vehicles with users on-board (blue) and rebalancing vehicles without users on-board (red) for 2-seater (2s), 4-seater (4s) and 4-seater+ (4s+) in Manhattan, with ride-pooling (rp) and without it. Maximum waiting time and delay are set to $\bar{t}, \bar{\delta} = 10$ min, respectively. The maximum number of users that can be ride-pooled together at the same time is $K = 2$ for every vehicle. Number of travel demands equals to 14 thousand per hour.

seater overcomes the drawbacks of having less user seats. Conversely, for a higher waiting time and number of travel requests, the higher energy consumption of a larger vehicle is counterbalanced by the possibility of efficiently pooling together more than two users. To conclude, these results show that the best vehicle choice is strongly influenced by some parameters, like waiting time and number of requests, and that, in ride-pooling systems energy consumption can be outweighed by the number of user seats in the vehicle. In a densely populated area like Manhattan, where there is a large number of travel requests per unit time, it is convenient to have a larger vehicle with lower energy efficiency per unit distance but more seats, i.e., a 4-seater shall be preferred over a 2-seater.

4. Conclusion

This paper proposed a modeling and optimization framework to jointly optimize operations and charging infrastructure design for Electric Autonomous Mobility-on-Demand (E-AMoD) systems with ride-pooling in a computationally tractable, scalable and globally optimal fashion. We devised a time-invariant network flow model that accounts for the State of Charge (SoC) of the vehicles, without the actual fleet size affecting its computational complexity. Leveraging this model, we formulated the ride-pooling E-AMoD joint operation and infrastructure problem as a mixed-integer linear program that can be solved with global optimality guarantees using off-the-shelf optimization algorithms. Our case study showed that jointly optimizing the charging infrastructure placement optimally can improve the performance achievable by the E-AMoD system by approximately 1%. In addition, we showed ride-pooling can significantly decrease energy consumption, with an improvement of up to 45% for densely populated urban environments. Lastly, we showed that the optimal choice of the vehicles is strongly

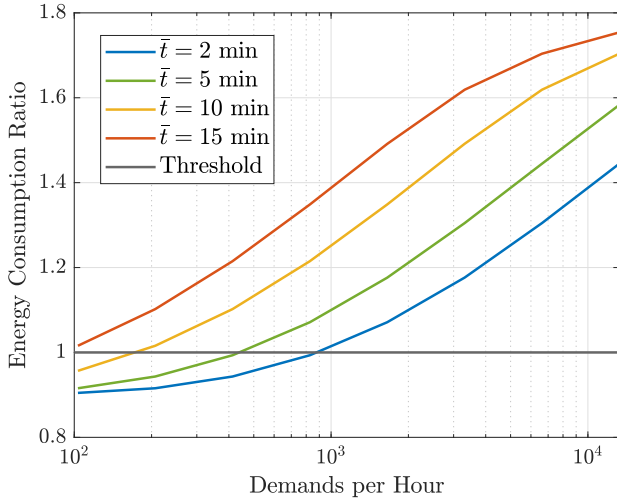


Figure 7: Energy consumption ratio between a fleet of 2-seaters and 4-seaters, with a maximum delay set to $\bar{\delta} = 10$ min. Above 1000 demands per hour, using heavier 4-seater is more energy efficient even for low waiting times \bar{t} of 2 min only.

influenced by the number of users in the systems and waiting time. For the case study of Manhattan, using 4-seaters appeared to be more beneficial albeit their higher energy consumption, as it allows to efficiently pool together more than two users.

For future work, we would like to take into account the total costs of ownership of the fleet, and the costs for the charging infrastructure and its capacity; study intermodal settings (Salazar et al., 2020; Wollenstein-Betech et al., 2021); and include incentives for ride-pooling (Fielbaum et al., 2022; Pedroso et al., 2023).

5. Acknowledgments

We thank Dr. I. New for proofreading the paper. This publication is part of the project NEON with number 17628 of the research program Crossover.

References

Alizadeh, M., Wai, H.T., Scaglione, A., Goldsmith, A., Fan, Y.Y., Javidi, T., 2014. Optimized path planning for electric vehicle routing and charging, in: Allerton Conf. on Communications, Control and Computing.

Alonso-Mora, J., Samaranayake, S., Wallar, A., Frazzoli, E., Rus, D., 2017. On-demand high-capacity ride-sharing via dynamic trip-vehicle assignment. *Proceedings of the National Academy of Sciences* 114, 462–467. doi:10.1073/pnas.1611675114.

Banerjee, S., Johari, R., Riquelme, C., 2015. Pricing in ride-sharing platforms: A queueing-theoretic approach, in: *ACM Conf. on Economics and Computation*.

Bertucci, J., Hofman, T., Salazar, M., 2024. Joint optimization of charging infrastructure placement and operational schedules for a fleet of battery electric trucks, in: *American Control Conference*. Available online at <https://arxiv.org/abs/2310.02181>.

Boewing, F., Schiffer, M., Salazar, M., Pavone, M., 2020. A vehicle coordination and charge scheduling algorithm for electric autonomous mobility-on-demand systems, in: *American Control Conference*.

Bullo, F., 2020. *Lectures on Network Systems*. 1.4 ed., Kindle Direct Publishing. Available online at <http://motion.me.ucsb.edu/book-1ns>, with contributions by J. Cortes, F. Dorfler, and S. Martinez.

Estandia, A., Schiffer, M., Rossi, F., Luke, J., Kara, E.C., Rajagopal, R., Pavone, M., 2021. On the interaction between autonomous mobility on demand systems and power distribution networks—an optimal power flow approach. *IEEE Transactions on Control of Network Systems* 8, 1163–1176. doi:10.1109/TCNS.2021.3059225.

Fielbaum, A., Kucharski, R., Cats, O., Alonso-Mora, J., 2022. How to split the costs and charge the travellers sharing a ride? aligning system’s optimum with users’ equilibrium. *European Journal of Operational Research* 301, 956–973. doi:<https://doi.org/10.1016/j.ejor.2021.11.041>.

Hogeveen, P., Steinbuch, M., Verbong, G., Hoekstra, A., 2021. Quantifying the fleet composition at full adoption of shared autonomous electric vehicles: An agent-based approach. *The Open Transportation Journal* 15, 47–60.

Hoppe, H., Enders, T., Cappart, Q., Schiffer, M., 2024. Global rewards in multi-agent deep reinforcement learning for autonomous mobility on demand systems. Available online at: <https://arxiv.org/abs/2312.08884>.

Iglesias, R., Rossi, F., Zhang, R., Pavone, M., 2019. A BCMP network approach to modeling and controlling autonomous mobility-on-demand systems. *Proc. of the Inst. of Mechanical Engineers, Part D: Journal of Automobile Engineering* 38, 357–374.

Le Floch, C., di Meglio, F., Moura, S., 2015. Optimal charging of vehicle-to-grid fleets via pde aggregation techniques, in: *Proc. of the American Nuclear Conference*. doi:10.1109/ACC.2015.7171839.

Levin, M.W., Kockelman, K.M., Boyles, S.D., Li, T., 2017. A general framework for modeling shared autonomous vehicles with dynamic network-loading and dynamic ride-sharing application. *Computers, Environment and Urban Systems* 64, 373 – 383.

Lightyear, 2016. Available online at <https://lightyear.one/> Accessed: 26/09/2022.

Luke, J., Salazar, M., Rajagopal, R., Pavone, M., 2021. Joint optimization of electric vehicle fleet operations and charging station siting, in: *Proc. IEEE Int. Conf. on Intelligent Transportation Systems*.

Neuburger, H., 1971. The economics of heavily congested roads. *Transportation Research* 5, 283–293.

Paparella, F., Chauhan, K., Hofman, T., Salazar, M., 2023. Electric autonomous mobility-on-demand: Joint optimization of routing and charging infrastructure siting, in: *IFAC World Congress*.

Paparella, F., Hofman, T., Salazar, M., 2024a. Electric autonomous mobility-on-demand: Jointly optimal vehicle design and fleet operation. *IEEE Transactions on Intelligent Transportation Systems Under Review*.

Paparella, F., Pedroso, L., Hofman, T., Salazar, M., 2024b. Congestion-aware ride-pooling in mixed traffic for autonomous mobility-on-demand systems, in: *European Control Conference*. In Press, Available online at <https://arxiv.org/abs/2311.03268>.

Paparella, F., Pedroso, L., Hofman, T., Salazar, M., 2024c. A time-invariant network flow model for ride-pooling in mobility-on-demand systems. *IEEE Transactions on Control of Network Systems Under Review*.

Pavone, M., 2015. *Autonomous Mobility-on-Demand systems for future urban mobility*, in: *Autonomes Fahren*. Springer.

Pavone, M., Smith, S.L., Frazzoli, E., Rus, D., 2012. Robotic load balancing for Mobility-on-Demand systems. *Proc. of the Inst. of Mechanical Engineers, Part D: Journal of Automobile Engineering* 31, 839–854.

Pedroso, L., Heemels, W.P.M.H., Salazar, M., 2023. Urgency-aware routing in single origin-destination itineraries through artificial currencies, in: *Proc. IEEE Conf. on Decision and Control*.

Rossi, F., Iglesias, R., Alizadeh, M., Pavone, M., 2020. On the interaction between Autonomous Mobility-on-Demand systems and the power network: Models and coordination algorithms. *IEEE Transactions on Control of Network Systems* 7, 384–397.

Rossi, F., Iglesias, R., Zhang, R., Pavone, M., 2017. Congestion-aware randomized routing in autonomous mobility-on-demand systems. Extended version Available at https://asl.stanford.edu/wp-content/papercite-data/pdf/Rossi_Iglesias_Zhang_Pavone_CDC17.pdf.

Sadri, A., Salim, F.D., Ren, Y., Zameni, M., Chan, J., Sellis, T., 2017. Shrink: Distance preserving graph compression. *Information Systems* 69, 180–193. doi:<https://doi.org/10.1016/j.is.2017.06.001>.

Salazar, M., Lanzetti, N., Rossi, F., Schiffer, M., Pavone, M., 2020. Intermodal autonomous mobility-on-demand. *IEEE Transactions on Intelligent Transportation Systems* 21, 3946–3960.

Santi, P., Resta, G., Szell, M., Sobolevsky, S., Strogatz, S.H., Ratti, C., 2014. Quantifying the benefits of vehicle pooling with shareability networks. *Proceedings of the National Academy of Sciences* 111, 13290–13294.

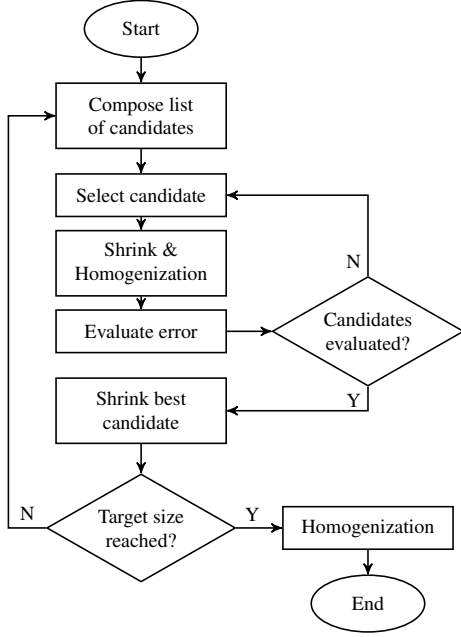


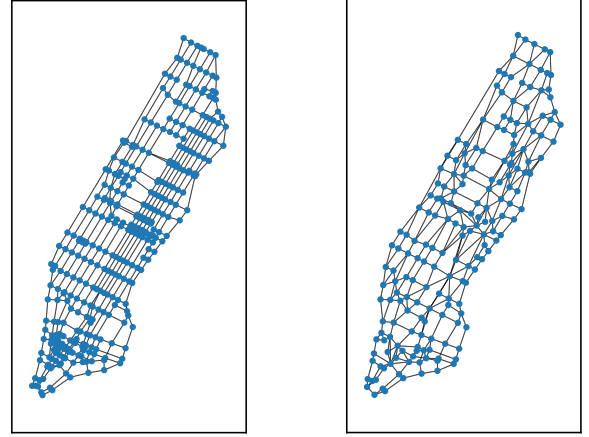
Figure A.8: Flow chart of the algorithm used to create the synthetic network in Fig. 2, where "Shrink" refers to the algorithm devised in Sadri et al. (2017).

- Spieser, K., Treleven, K., Zhang, R., Frazzoli, E., Morton, D., Pavone, M., 2014. Toward a systematic approach to the design and evaluation of Autonomous Mobility-on-Demand systems: A case study in Singapore, in: Road Vehicle Automation. Springer.
- Turan, B., Tucker, N., Alizadeh, M., 2019. Smart charging benefits in autonomous mobility on demand systems, in: Proc. IEEE Int. Conf. on Intelligent Transportation Systems.
- Vehlhaber, F., Salazar, M., 2023. Electric aircraft assignment, routing, and charge scheduling considering the availability of renewable energy. IEEE Control Systems Letters 7, 3669–3674. doi:10.1109/lcsys.2023.3339998. available online at <http://arxiv.org/pdf/2309.09793v1>.
- Wang, R., Zeng, T., Keyantuo, P., Sandoval, J., Vishwanath, A., Borhan, H., Moura, S., 2023. Optimal Dispatch and Routing of Electrified Heavy-Duty Truck Fleets: A Case Study with Fleet Data, in: IEEE Control Systems Letters.
- Wollenstein-Betech, S., Salazar, M., Houshmand, A., Pavone, M., Cassandras, C.G., Paschalidis, I.C., 2021. Routing and rebalancing intermodal autonomous mobility-on-demand systems in mixed traffic. IEEE Transactions on Intelligent Transportation Systems 23, 12263–12275.

Appendix A. Iso-energy Pruning of the Road Network

In this section we explain the algorithm used to create, starting from the original road network, a new synthetic road network with iso-energy arc weights in terms of energy consumption. We leverage the Shrink method devised by Sadri et al. (2017). Compared to the original formulation, we modify the algorithm by expanding the node selection procedure to every node and merging the two nodes such that the absolute difference between all the adjacent arcs w.r.t. the two nodes and the target weight (or a multiple integer of the target weight) is minimized. Fig. A.8 shows the flowchart of the algorithm based on Shrink. We refer the reader to the paper written by Sadri et al.

(2017) for a detailed analysis of the algorithm. Our results of Manhattan, NYC, show that when applying the algorithm described above, there is a correlation between the desired compression rate, the optimal target weight and the average absolute



(a) Original road network of Manhattan, (b) Synthetic road network of Manhattan, NYC for $w_c = 50$ Wh.

Figure A.9: Original road network and synthetic one of Manhattan, NYC. In the synthetic network, each arc might be split into several arcs of weight equal to the target one. Such sub-division is not represented in the figure.

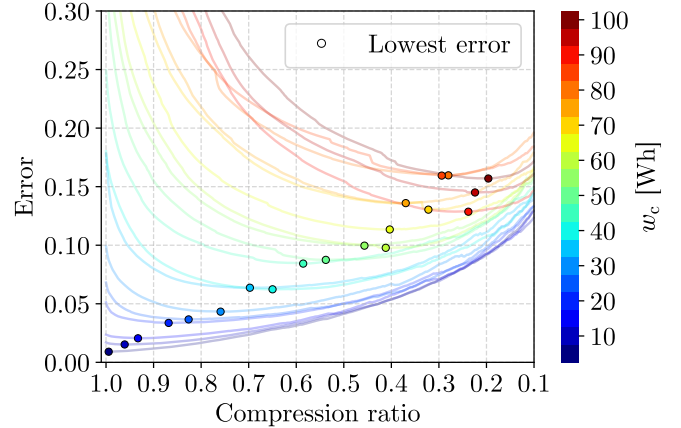


Figure A.10: Average absolute error of the shortest path between every node in the network as a function of the target weight and compression ratio. Results obtained for the network of Manhattan, NYC.

error of the shortest path for every couple of nodes. In particular, Fig. A.10 shows the relation between the quantities mentioned previously, and highlights that for a given compression ratio, there is a target weight which minimizes the expected error. Fig. A.9 shows an example of the difference between an original network and a synthetic one generated with the method presented. Note that in the figure, each arc might be split into multiple arcs in series so that the total weight is an integer multiple of the target weight. Such arcs in series are not depicted in the figure.